The Janus kinase inhibitor Ruxolitinib reduces HIV replication in human macrophages and ameliorates HIV encephalitis in a murine model

Woldeab B. Haile[3,§], **Christina Gavegnano**[1,3,§], **Sijia Tao**[1,3], **Yong Jiang**[1], **Raymond F. Schinazi**[1,3,*], and **William R. Tyor**[2,3,*]

[1]Center for AIDS Research, Laboratory of Biochemical Pharmacology, Department of Pediatrics, Emory University, Atlanta, GA 30322, USA

[2]Department of Neurology, Emory University School of Medicine, Atlanta, GA 30209, USA

[3]Veterans Affairs Medical Center, Decatur, GA 30033, USA

Abstract

A hallmark of persistent HIV-1 infection in the central nervous system is increased activation of mononuclear phagocytes and surrounding astrogliosis, conferring persistent HIV-induced inflammation. This inflammation is believed to result in neuronal dysfunction and the clinical manifestations of HIV-associated neurocognitive disorders (HAND). The Jak/STAT pathway is activated in macrophages/myeloid cells upon HIV-1 infection, modulating many pro-inflammatory pathways that result in HAND, thereby representing an attractive cellular target. Thus, the impact of ruxolitinib, a Janus Kinase (Jak) 1/2 inhibitor that is FDA approved for myelofibrosis and polycythemia vera, was assessed for its potential to inhibit HIV-1 replication in macrophages and HIV-induced activation in monocytes/macrophages in culture. In addition, a murine model of HIV encephalitis (HIVE) was used to assess the impact of ruxolitinib on histopathological features of HIVE, brain viral load, as well as its ability to penetrate the blood-brain-barrier (BBB). Ruxolitinib was found to inhibit HIV-1 replication in macrophages, HIV-induced activation of monocytes (CD14/CD16) and macrophages (HLA-DR, CCR5, and CD163) without apparent toxicity. *In vivo*, systemically administered ruxolitinib was detected in the brain during HIVE in SCID mice and markedly inhibited astrogliosis. Together, these data indicate that ruxolitinib reduces HIV-induced activation and infiltration of monocytes/macrophages *in vitro*, reduces the replication of HIV *in vitro,* penetrates the BBB when systemically administered in mice and reduces astrogliosis in the brains of mice with HIVE. These data suggest that ruxolitinib will be useful as a novel therapeutic to treat humans with HAND.

[*]Co-Corresponding authors, Dr, William R. Tyor:, Neurology (GECL), Atlanta VAMC, 1670 Clairmont Rd., Decatur, GA 30033; wtyor@emory.edu. Dr. Raymond Schinazi, Emory University, 1760 Haygood Drive, Suite E420, Atlanta, GA 30322, USA, Tel: +1-404-727-1414; rschina@emory.edu.
[§]equal contribution by each author

Introduction

With the introduction of combined antiretroviral therapy (ART), the neurocognitive dysfunction seen during HIV infection underwent a fundamental change. The incidence of HIV associated dementia was substantially reduced, but other milder forms of HIV associated neurocognitive disorders (HAND) have been recognized in approximately 40% to 50% of people living with HIV (PLHIV) (Rumbaugh and Tyor, 2015). These milder forms of HAND, which include asymptomatic neurocognitive impairment and mild neurocognitive disorder, can be found in PLHIV even when they are receiving ART.

It has become increasingly clear that standard ART will not eradicate HIV from the CNS. With an aging population of PLHIV who are more vulnerable to cognitive disorders, the combination of older age plus the chronic presence of HIV in the brain appears to result in a higher prevalence of milder forms of HAND, but of even more concern is evidence that these patients are probably more susceptible to increasing cognitive dysfunction (Grant et al., 2014). ART had no effect either way, although there has also been concern that certain ART regimens could be neurotoxic (Robertson et al., 2010). At any rate, the above implications emphasize the critical need to develop alternative approaches to therapy for HAND.

In order to gain insight into pathogenesis of HAND and help develop alternative treatments, our group developed a model of HIV encephalitis (HIVE) in SCID mice whereby HIV-infected or uninfected (controls) human monocytes are injected into the right frontal lobe (Tyor et al., 1993). Later these mice were shown to develop mild behavioral abnormalities suggesting it is a model for the milder forms of HAND (Avgeropoulos et al., 1998a). We have since shown that two different ART regimens do not eradicate HIV from the CNS, although they are somewhat effective at ameliorating histopathological features of HIVE (Cook et al., 2005; Koneru et al., 2014). We have also used this model to investigate novel treatments for HAND (Fritz-French et al., 2014).

In this paper, the effects of ruxolitinib (Jakafi®), a Jak/STAT inhibitor, on HIVE in SCID mice were investigated. HIV activates multiple Jak/STAT proteins that also activate mononuclear phagocytes (Rivera-Rivera et al., 2012). Additionally, HIV-induced inflammation conferred by activation of the Jak-STAT pathway can modulate a variety of factors impacting CNS infection, including priming of uninfected bystander cells for infection, recruitment of uninfected cells to the site(s) of infection, increased production of virus per infected cell, reactivation of latent virus from viral reservoirs/sanctuaries, promotion of global immune dysfunction that drives viral persistence across many tissues and sites simultaneously, and activation of infected monocytes, resulting in increased trafficking across the blood brain barrier (BBB), which promotes HIV associated neurocognitive impairments (Bovolenta et al., 1999; Dunfee et al., 2006; Lichtfuss et al.; M Chevalier1, 2013; Sippy et al., 1995; Thames et al., 2014). Based on this complex interplay of HIV-induced signaling events, many of which are driven by Jak-STAT signaling, it is plausible that selective, targeted inhibition of the Jak-STAT pathway could represent an attractive mechanism to truncate HIV-driven immunomodulation that impacts HAND. Mononuclear phagocytes are the key population of cells in the CNS that are infected by HIV

and also mediate inflammation in humans with HIVE (Glass et al., 1995) and also in our model (Tyor et al., 1993; Avgeropoulos et al., 1998a; Sas et al., 2009). Therefore, we hypothesized that interfering with Jak/STAT using ruxolitinib would improve one or more features of HIVE in the model and also possibly inhibit HIV in mouse brains. We found that systemically administered ruxolitinib was detected in the brain during HIVE in SCID mice and markedly inhibited astrogliosis. There appeared to be trends for improvement in mouse mononuclear phagocyte reaction during HIVE, improvement of neuronal dendritic arborization and decrease in HIV staining of human macrophages in the SCID mice treated with high dose ruxolitinib.

Methods

In vitro treatment of monocytes or macrophages with ruxolitinib and HIV-1

Macrophages and monocytes were isolated as previously described (Gavegnano et al., 2013). Cells were treated with various concentrations of ruxolitinib for 2 hr prior to infection (HIV-1$_{baL}$). Cells were maintained for 6 days before viral quantification (p24-ELISA). For *in vitro* activation marker studies, CD14$^+$ monocytes, or fully differentiated (CD14$^-$/CD11b$^+$) macrophages were used. Monocytes were used as a model to mimic HIV-induced activation that transpires in the periphery, wherein presence or internalization of HIV-1 in monocytes confers activation (CD14$^+$/CD16$^+$), and subsequent trafficking of "Trojan horse" monocytes across and within the BBB. The method used to differentiate macrophages (CD14$^-$/CD11b$^+$) has been validated by our group to ensure that these cells are no longer expressing monocyte marker CD14, and are mature macrophages (CD11b expression). The *in vitro* and *in vivo* work with macrophages were performed with cells prepared and validated in this manner. Macrophages or monocytes were treated with various concentrations of drug prior to infection (HIV-1$_{baL}$), and maintained for 3 or 6 days before quantification of HLA-DR, CD163, CCR5 (macrophages), or CD14/CD16 (monocytes); Miltenyi Biotec, San Diego, CA. Macrophages and monocytes were treated with various concentrations of drug for 6 days and stained with Near-IR live/dead dye and quantified by FACS. Antiviral potency was calculated as previously described (Gavegnano et al., 2013).

In vitro cytotoxicity

The median inhibitory concentration (IC$_{50}$) was determined by Zombie Violet stain (BioLegend, San Diego, CA) according to manufacturer's protocol (flow cytometry, Violet laser, 405 excitation/450 emission). For all assays, cells were cultured as described above and maintained in various concentrations of drug-containing medium for 6 days prior to assessment of toxicity. Cytotoxicity was considered when the concentrations of the test compounds alone inhibited growth by 50%. Gating strategy based on forward scatter (FSC) and side scatter (SSC) was established, followed by a sub gate for doublet discrimination. Additional negative control of cells incubated at various concentrations of AZT, which is known to be non-toxic to macrophages and monocytes, was used as a negative control, and a dose response of Cycloheximide (protein synthesis inhibitor additional positive control of cells exposed to various concentrations of cycloheximide, demonstrated a dose response of toxicity; data not shown. Gating was established based on viable cells cultured in the absence of drug. Data are represented in Supplemental Figure 1.

Human Monocytes and HIV-1$_{ADA}$

Human monocyte-derived macrophages (MDMs) were cultured and infected as described in our previous reports (Cook-Easterwood et al., 2007; Sas et al., 2009). Briefly, primary human monocytes and HIV-1$_{ADA}$ were obtained from Dr. Howard Gendelman, University of Nebraska Medical Center, Omaha, NE. Control and HIV-infected monocytes cells were stimulated with 7 ng/ml macrophage colony-stimulating factor for 7 days, followed by HIV-1 infection at MOI of 0.1, for 2 more weeks to allow for sufficient infection of at least 50% of the cells. MDMs were collected and re-suspended in sterile phosphate-buffered saline (PBS) for intracranial (IC) inoculation.

Animals and inoculation

Five-week-old B6.CB17-Prkdcscid/SzJ male mice were obtained from the Jackson Laboratory. All procedures were approved by the Institutional Animal Care and Use Committee of the Atlanta Veterans Administration Medical Center and were in accordance with the guidelines of the NIH Guide for the Care and Use of Laboratory Animals (NIH Publication No. 80-23, revised 1996). Mice were intracerebrally (IC) inoculated either with 10^5 HIV-infected or uninfected control human MDMs re-suspended in 30μL PBS into the right frontal lobe under xylazine (5 mg/kg) and ketamine (95 mg/kg) anesthesia. IC inoculations were performed using a syringe fitted with a collar guard to control depth to 3.5 mm below the skull surface.

Treatment Groups

In the course of the 10-day infection period, experimental mice received saline, low dose ruxolitinib, high dose ruxolitinib or tenofovir by subcutaneous (SQ) injection whereas control mice received 100 μL of saline. HIV-infected mice were separated into four groups of six mice each. The first group received 100 μL of saline three times daily, the second group received low dose ruxolitinib (20 mg/kg per injection) in 100 μL of saline two times per day (BID), the third group received high dose ruxolitinib (50 mg/kg per injection) in 100 μL of saline three times per day (TID) and the fourth group received 75 mg/kg per injection of tenofovir TID, based on dosing in a previously published study (Koneru et al., 2014). Preliminary data indicated the plasma half-life of ruxolitinib, as measured by mass spectroscopy, to be approximately 2–3 hours and hence the TID dosage. Mice were monitored for physical and behavioral changes and showed no signs of toxicity. Physical parameters monitored included weight, appearance of fur and ear positioning, and appearance of injection area. To monitor behavior, the mice were given fresh bedding daily to ensure that they were shredding and their level of lethargy was assessed. Food and water intake were normal as assessed daily.

Immunohistochemistry

At day 10 post IC-inoculation, all mice were sacrificed under xylazine (5 mg/kg) and ketamine (95 mg/kg) anesthesia and brains were extracted, snap-frozen in tissue-freezing medium, and stored at −70°C until cryosectioning. Tissue sectioning and immunohistochemistry were performed as described previously (Sas, 2007). Five μm coronal brain sections were taken beginning at the rostral end of the prefrontal cortex at 250

µm intervals antero-posteriorly. Since injections are done manually, the general site of injection falls in the cortical region spanning between 1.5 mm to 2.5 mm anterior to bregma, which is mainly in the frontal lobe. Cryosectioned tissues were then stained using an immunoperoxidase method as previously described (Avgeropoulos et al., 1998b). In brief, sections were stained for mouse microglia and macrophages (1:50 CD45; AbD Serotec), HIV (1:50 p24; Dako), astrogliosis [1:750 glial fibrillary acidic protein (GFAP); Chemicon], and neuronal dendrites (1:200 microtubule-associated protein-2 (MAP2); Chemicon). Slides were then reviewed under a light microscope (Olympus Microscope).

Densitometry scoring

The optical density was obtained as follows: 10 X (GFAP), 20 X (CD45) and 40 X (MAP2) and images were captured using an Olympus DP80 digital camera attached to an Olympus BX51 microscope. Images were then analyzed by Image J 1.45S software (NIH). Microscope and image capture parameters were kept constant. Each slide was subjected to the Image J software by selecting the representative GFAP or CD45 positive area and adjustments were made to include all GFAP and CD45-positive staining. We have kept image gain constant for all sections stained for the same protein marker. However, in order to make sure that data reflected only positive staining and not background staining, threshold adjustments were needed to be made between different markers, such as GFAP and CD45 depending on the intensity of the staining. For example, GFAP antibody staining is relatively more intense compared to CD45, therefore, the use of different gain was necessary. Artifactual signals such as empty ventricles or folded tissue were not measured. For MAP2 staining, mean optical density in the uninjected hemisphere (left) was assigned as a control for the injected hemisphere (right). The intensity of signal was measured in both the uninjected and injected hemispheres and the percent reduction in MAP2 staining in the injected hemisphere in relation to the uninjected hemisphere was considered a surrogate for the percent reduction in dendritic arborization. The evaluator was blinded to treatment when performing densitometry scoring.

P24 measurement

P24 positive cells were manually counted in all the sections taken at 250 µm intervals beginning at the anterior tip of the prefrontal cerebral cortex. A total of 10 sections were taken for the analysis, spanning a total of about 2.5 mm into the frontal cortex. The evaluator was blinded to treatment when counting p24 positive cells.

Ruxolitinib extraction and quantification

In order to measure levels of Ruxolitinib in the brain, mice underwent cardiac perfusion with PBS prior to brain extractions. After brain extraction, posterior fossa (the cerebellum and brainstem) was taken, snap frozen and stored at −70 °C. Posterior fossa from each mouse was then weighed and homogenized in water:methanol (2:1) solution. The homogenates were then centrifuged and the pellet discarded. The supernatant was dried by evaporation using nitrogen gas, resuspended in 1 mL water and put through Isolute-XL C18 columns (Biotage, Uppsala, Sweden). Drug was then eluted with acetonitrile and subsequently dried. Finally, samples were resuspended in 1 mL of 75% methanol (containing 0.1% formic acid)

and ruxolitinib levels were measured by liquid chromatography and tandem mass spectrometry (LC-MS/MS).

Liquid Chromatograph and Tandem Mass Spectrometry (LC-MS/MS)

Chromatographic separation was performed by Ultimate 3000 LC system (Thermo Scientific, MA, USA), on a Kinetex XB-C18 column (50 × 2.1 mm) with a 2.6 μm particle size (Phenomenex, CA, USA). The mobile phase A consisted of 0.1% formic acid in water and the mobile phase B consisted of methanol. Isocratic elution was used for the separation with mobile phase A:B at 25:75 (v/v). The column was maintained at ambient temperature. The flow rate was maintained at 250 μL/min and a 20 μL injection was used. An API5000 triple quadrupole mass spectrometer (ABsciex, MA, USA.) was used for detection, with electrospray ionization in positive ion mode. The mass spectrum parameters for the analytes were set as follows: ion spray voltage, 5500 V; curtain gas, 25 psi; ion source gas 1, 40 psi; ion source gas 2, 40 psi; source temperature, 500 °C and collision gas, 5 psi. Multiple reaction monitoring transitions for ruxolitinib was m/z 307.3 → 186.0 and for baricitinib (internal standard) m/z 372.2 → 186.0. Analyst software version 1.5.2 was used to operate the mass spectrometer and to perform data analysis. Calibration curves were generated from standard of ruxolitinib by serial dilutions in blank mouse brain samples using the same extraction method described above. The calibration curves had r^2 value greater than 0.99.

Statistics

Analyses of densitometry values were performed using 1-way ANOVA and an unpaired t-test in GraphPad Prism 5 for Windows (GraphPad Software). Significance was set at *=p<0.05 and **=p<0.01 for all analyses. Statistical analysis of activation markers were performed using a One Way ANOVA followed by a post-hoc test, where p < 0.05 was considered statistically significant. T-test was used to compare the mean numbers of p24 positive monocytes between saline and ruxolitinib treated HIV-infected mice. Six mice were used for each treatment condition. .

Results

Antiviral potency and toxicity of ruxolitinib in primary human lymphocytes and macrophages

Ruxolitinib was not cytotoxic (> 50 μM for ruxolitinib) in primary human macrophages, and antiviral potency was 0.3 ± 0.1 μM (median effective concentration or EC_{50}) and 3.1 ± 1.8 (90% effective concentration or EC_{90}) in macrophages (Supplemental Table 1). As expected, AZT control demonstrated submicromolar antiviral potency. Therapeutic window of safety (ratio of toxicity:potency) was > 100 for ruxolitinib, demonstrating that observed effects are a function of anti-HIV effects of ruxolitinib and not toxicity (Gavegnano, C., et al., 2014).

Ruxolitinib inhibited HIV-induced activation in primary human macrophages and monocytes

Ruxolitinib conferred a dose dependent reduction of activation markers HLA-DR, CD163, CCR5 (macrophages), and CD14/CD16 (monocytes) that were up-regulated by HIV-1 infection in primary human macrophages and monocytes (Figure 1A and B). Data reported

are normalized to percent of expression *versus* no drug controls, wherein original starting percentage of $CD14^+/CD16^+$ monocytes exposed to HIV-1 were 62 ± 4.6 %, and 51 ± 3.9 % for macrophages.

Ruxolitinib crosses the blood brain barrier (BBB)

Ruxolitinib was found to cross the BBB and enter the brain parenchyma following SQ injection of the higher dose (50 mg/kg/injection). Levels of ruxolitinib were measured in the brain parenchyma by mass spectroscopy 1 hr after the last injection. Ruxolitinib was detected in the brains of all 6 mice used in this study (Table 1). The average level of ruxolitinib in the mouse- brain, was 137.7 ng/g of brain tissue.

Ruxolitinib decreases encephalitis markers

High dose ruxolitinib (50 mg/kg per injection TID) completely abrogated astrogliosis induced by HIV infection (Figures 2A and 3C). GFAP densitometry decreased by 60% in the high dose ruxolitinib group compared to the HIV saline group and was comparable to the levels of the uninfected control mice. High dose ruxolitinib treatment also showed a decrease in p24 positive human macrophages counted (Figures 2B and 3D–F), a reversal in HIV mediated increase in mononuclear phagocyte staining (Figures 2C and 3G–I), and an improvement in neuronal arborization as evidenced by an increase in MAP-2 staining (Figure. 2D and 3J–L), in mice that received high dose ruxolitinib. However, these observations did not reach statistical significance with p values of 0.24, 0.21 and 0.23 respectively.

Low dose treatment of ruxolitinib (20 mg/kg per injection BID) also showed a statistically significant decrease in astrogliosis compared to HIVE mice receiving saline, (p=0.007) (Figure 2E). However, it failed to show any trend in other encephalitis markers. An antiretroviral drug, tenofovir, also resulted in 69% reduction in astrogliosis compared to saline treated group (p=0.0001). In addition, tenofovir showed a decrease in the average viral load but did not reach statistical significance (p=0.28). There were no observable trends in CD45 and MAP-2 staining after treatment with tenofovir.

Discussion

Our studies demonstrated *in vitro*, where direct consideration for the impact of ruxolitinib on the dynamics of HIV and monocytes/macrophages can be observed, that ruxolitinib was a submicromolar inhibitor of HIV replication in macrophages without apparent toxicity. Ruxolitinib significantly reduced (p < 0.05) HIV-induced activation markers (monocytes/ macrophages; CD14/CD16, HLA-DR, CCR5, CD163), which are linked to trafficking of infected cells to the CNS, disease progression, and neurocognitive dysfunction. Our group has previously reported the toxicity profile for ruxolitinib in primary human cells, including lymphocytes and macrophages (Gavegnano et al, 2013). These results, along with toxicity in monocytes are summarized in Supplemental Table 1. The therapeutic window (ratio of potency:toxicity) for the observed antiviral and inhibition of pro-HIV events is > 100 for ruxolitinib in monocytes, macrophages, and lymphocytes. Additionally, the FDA submission information for ruxolitinib contains extensive *in vitro* and *in vivo* toxicity studies,

demonstrating that ruxolitinib is not toxic up to 100 μM *in vitro*, and that its *in vivo* peak and steady-state plasma concentrations for FDA approved doses are above the concentrations required to confer anti-HIV properties in the assays reported herein. Therefore, we are confident that the observed results are a function of the Jak1/2 inhibition conferred by ruxolitinib, and not toxicity.

Regarding *in vivo* murine studies, the plasma pharmacokinetics (PK) coupled with the pharmacodynamic (PD) profile *in vivo* is reported (Chen et al., 2013; Verstovsek et al., 2012), and are also summarized in the ruxolitinib package insert (Jakafi.com). To assess PK/PD relative to the *in vitro* and *in vivo* efficacy reported herein, baseline PPK model parameters (Chen et al., 2013 and Verstovsek et al, 2012; without explicit patient covariates) were used to construct our PPK model. Our model used ω^2 as the $\leftrightarrow$ subject variance (IIV) for that PK parameter, and σ^2 = residual variance (within subjects). Log-normal error structure (e.g. CL/Fi = CL/F "typical" $\times e^{\eta_i}$ η_i are N(0, ω^2) i.e., %CV = (e − 1) × 100 was used and 1,000 theoretical participants administered 10 mg ruxolitinib twice per day were modeled. Resulting computed percentile (P_{10}, P_{25}, P_{50} P_{75}, P_{90}) plasma concentrations versus time were used to mimic *in vivo* doses of 10 mg and 25 mg bid, which are the low and high FDA-approved doses. Our model demonstrated that the PD effect of ruxolitinib falls within the C_{max} and steady-state range for all FDA approved doses of ruxolitinib.

Ruxolitinib was found to cross the BBB when administered to mice systemically as measured by tandem mass spectroscopy in the brain fossa. The brain fossa was selected for the measurement of ruxolitinib because previous work in our laboratory, using antiretroviral drugs, has shown a uniform distribution of the drugs within the different compartments of the brain (Cook et al., 2005) And since the majority of the brain tissue was used for histopathological analysis, the brain stem and cerebellum were necessarily used as representative regions to measure drug levels. In light of the CNS effects of ruxolitinib on astrogliosis in HIVE mice, the detection of ruxolitinib in the brain is not surprising. However, a European review for approval in humans states that ruxolitinib could not be detected in the brains of rats systemically administered the drug using whole body autoradiography (http://ec.europa.eu/health/documents/community-register/ 2012/20120823123254/anx_123254_en.pdf). We believe this method of detection (i.e., whole body radiation) is not as sensitive as our use of brain parenchymal mass spectroscopy analysis. In addition, a Canadian review for approval of ruxolitinib for use in humans states that "Ruxolitinib and its metabolites crossed the blood brain barrier (<10% of plasma concentrations) and placental barrier of rats" (http://www.hc-sc.gc.ca/dhp-mps/prodpharma/ sbd-smd/drug-med/sbd_smd_2012_jakavi_151723-eng.php). Although these data do not necessarily predict that the drug will cross the BBB in humans, the fact that the potential population involved, PLHIV with HAND, have mild encephalitis and may have an impaired BBB, lends further support for a trial in humans, which will be enrolling a phase 2a NIH-ACTG-sponsored study in 2015 to assess the impact of ruxolitinib on HIV-induced inflammation.

In vivo, ruxolitinib resulted in a significant reduction in astrogliosis. Astrogliosis is a common finding in HIVE in humans and correlates with neuropsychological impairment (Everall et al., 2009). Astrogliosis has been postulated to play a role in the pathogenesis of

HIVE (Schouten et al., 2011; Thompson et al., 2001). Furthermore, astrocytes are probably activated during CNS infection by HIV and they almost certainly are capable of producing many of the substances such as cytokines, chemokines and other potential neurotoxins that are implicated in HAND pathogenesis. In our model of HIVE in mice, astrogliosis is consistently, strongly induced by HIV infection and has previously been shown to be reduced by ART (Cook et al., 2005; Koneru et al., 2014). It was therefore somewhat surprising that ruxolitinib alone, either in low dose or high dose and without accompanying ART, showed substantially reduced astrogliosis in HIVE mice (Figures 2A and 3A–C). However, ruxolitinib inhibits Jak1, which has been shown to be activated in astrocytes following cerebral ischemia in rats (Justicia et al., 2000). Further, interferon-gamma (IFN-γ) production by many cell types, including astrocytes themselves, is regulated through this pathway. Stimulation of astrocytes by IFN-γ is known to result in the production of neurotoxins, which could be involved in HAND pathogenesis (Lee et al., 2013). It is therefore possible that the inhibitory effects of ruxolitinib in HIVE in mice could have important implications in the treatment of HAND in humans.

Ruxolitinib treatment in HIVE mice also showed a reduction in the average mouse mononuclear phagocyte numbers but did not reach statistical significance (p=0.2). As mentioned in the Introduction, mononuclear phagocytes are activated by HIV through Jak/STAT signaling and many cytokines that are produced during HIV infection signal through the Jak/STAT pathway (Rivera-Rivera et al., 2012). Mononuclear phagocytes are arguably the most important cell type implicated in HAND pathogenesis. That ruxolitinib likely has an inhibitory effect on these cells during HIVE in mice has potential important consequences for the effectiveness of Jak/STAT inhibitors in ameliorating human HAND, especially in those HIV-infected persons already receiving ART. Our data also suggest that there are positive effects of ruxolitinib on MAP2 staining (i.e., dendritic arborization), as shown by increased MAP-2 staining in the ruxolitinib treated mice compared to the saline controls, although it did not attain statistical significance (p=0.21). The fact that ruxolitinib treatment of our HIVE mice may also be improving the detrimental neuronal effects of HIV adds further credence to the idea that Jak/STAT inhibitors could be attractive choices as an add on treatment for HAND patients who are taking ART. We have previously shown that dendritic arborization, as measured by MAP2 immunostaining, correlates with behavioral analysis of HIVE mice (Cook-Easterwood et al., 2007; Sas et al., 2009). Therefore, ameliorating MAP2 abnormalities predicts improvement in behavior of HIVE mice. In the future we plan to test the effect of ruxolitinib on the behavior of HIVE mice. We predict behavior in the water radial arm maze will be improved with high dose ruxolitinib, which would validate the possible improvement in MAP2 staining and further suggest that ruxolitinib will improve cognitive deficits in HAND patients. These data are complimented by the observed decrease in p24^{+} cells in HIVE mice treated with high dose ruxolitinib and may be related to its effects on mononuclear phagocytes activation in the brain and/or effects on inhibition of HIV replication.

In summary, we have shown that *in vitro*, ruxolitinib inhibits HIV-induced activation of monocytes (CD14/CD16) and macrophages (HLA-DR, CCR5, and CD163). These markers are associated with trafficking of infected monocytes across and within the BBB, and are associated with HIV-induced neurocognitive dysfunction and impairments including HAND.

Additionally, ruxolitinib is a submicromolar inhibitor of HIV-1 replication in macrophages *in vitro,* without any apparent toxicity. When administered systemically to mice with HIVE, ruxolitinib crosses the BBB and has substantial effects on pathology, most notably the reduction of astrogliosis. The data further suggest that other possible effects on reducing mononuclear phagocyte numbers, preventing dendritic abnormalities that probably relate to cognitive dysfunction, and possibly reducing HIV CNS load are all positive effects that suggest ruxolitinib will be effective in humans with HAND.

Supplementary Material

Refer to Web version on PubMed Central for supplementary material.

Acknowledgments

References

Avgeropoulos N, et al. SCID mice with HIV encephalitis develop behavioral abnormalities. J Acquir Immune Defic Syndr Hum Retrovirol. 1998a; 18:13–20. [PubMed: 9593453]

Avgeropoulos NG, et al. Potential relationships between the presence of HIV, macrophages, and astrogliosis in SCID mice with HIV encephalitis. J NeuroAIDS. 1998b; 2:1–20. [PubMed: 16873182]

Bovolenta C, et al. Constitutive activation of STATs upon in vivo human immunodeficiency virus infection. Blood. 1999; 94:4202–9. [PubMed: 10590065]

Chen X, et al. Population pharmacokinetic analysis of orally-administered ruxolitinib (INCB018424 Phosphate) in patients with primary myelofibrosis (PMF), post-polycythemia vera myelofibrosis (PPV-MF) or post-essential thrombocythemia myelofibrosis (PET MF). J Clin Pharmacol. 2013; 53:721–30. [PubMed: 23677817]

Cook-Easterwood J, et al. Highly active antiretroviral therapy of cognitive dysfunction and neuronal abnormalities in SCID mice with HIV encephalitis. Exp Neurol. 2007; 205:506–12. [PubMed: 17442303]

Cook JE, et al. Highly active antiretroviral therapy and human immunodeficiency virus encephalitis. Ann Neurol. 2005; 57:795–803. [PubMed: 15852478]

Dunfee R, et al. Mechanisms of HIV-1 neurotropism. Curr HIV Res. 2006; 4:267–78. [PubMed: 16842080]

Everall I, et al. Cliniconeuropathologic correlates of human immunodeficiency virus in the era of antiretroviral therapy. J Neurovirol. 2009; 15:360–70. [PubMed: 20175693]

Fritz-French C, et al. The recombinant vaccinia virus gene product, B18R, neutralizes interferon alpha and alleviates histopathological complications in an HIV encephalitis mouse model. J Interferon Cytokine Res. 2014; 34:510–7. [PubMed: 24564363]

Gavegnano C, et al. Cellular pharmacology and potency of HIV-1 nucleoside analogs in primary human macrophages. Antimicrob Agents Chemother. 2013; 57:1262–9. [PubMed: 23263005]

Gavegnano C, et al. Ruxolitinib and tofacitinib are potent and selective inhibitors of HIV-1 replication and virus reactivation in vitro. Antimicrob Agents Chemother. 2014; 58(4):1977–86. 014. [PubMed: 24419350]

Glass JD, et al. Immunocytochemical quantitation of human immunodeficiency virus in the brain: correlations with dementia. Ann Neurol. 1995; 38:755–62. [PubMed: 7486867]

Grant I, et al. Asymptomatic HIV-associated neurocognitive impairment increases risk for symptomatic decline. Neurology. 2014; 82:2055–62. [PubMed: 24814848]

Justicia C, et al. Activation of the JAK/STAT pathway following transient focal cerebral ischemia: Signaling through Jak1 and Stat3 in astrocytes. Glia. 2000; 30:253–270. [PubMed: 10756075]

Koneru R, et al. Combined antiretroviral therapy reduces brain viral load and pathological features of HIV encephalitis in a mouse model. J Neurovirol. 2014; 20:9–17. [PubMed: 24415129]

Lee M, et al. Neurotoxins released from interferon-gamma-stimulated human astrocytes. Neuroscience. 2013; 229:164–75. [PubMed: 23098801]

Lichtfuss GF, et al. Virologically suppressed HIV patients show activation of NK cells and persistent innate immune activation. J Immunol. 189:1491–9. [PubMed: 22745371]

Chevalier, M., 1; Petitjean, G., 1; Didier, C., 1; Dunyach-Remy, C., 3,4; Girard, P-M., 5; Meyer, L., 6; Lavigne, J-P., 3,4; Barre-Sinoussi, F., 1; Scott-Algara, D., 1; Weiss, Laurence, *1,7,8. Soluble CD14 and IL-1ra Levels Predict the Immune Activation Set Point in the Absence of Microbial Translocation in Primary HIV Infection. 20th Conference on Retroviruses and Opportunistic Infections; Atlanta, GA. 2013;

Rivera-Rivera L, et al. Inhibition of interferon response by cystatin B: implication in HIV replication of macrophage reservoirs. J Neurovirol. 2012; 18:20–9. [PubMed: 22147503]

Robertson KR, et al. Neurocognitive effects of treatment interruption in stable HIV-positive patients in an observational cohort. Neurology. 2010; 74:1260–6. [PubMed: 20237308]

Rumbaugh JA, Tyor W. HIV-associated neurocognitive disorders: Five new things. Neurol Clin Pract. 2015; 5:224–231. [PubMed: 26124979]

Sas AR. Cognitive dysfunction in HIV encephalitic SCID mice correlates with levels of Interferon-alpha in the brain. AIDS. 2007

Sas AR, et al. Interferon-alpha causes neuronal dysfunction in encephalitis. J Neurosci. 2009; 29:3948–55. [PubMed: 19321791]

Schouten J, et al. HIV-1 infection and cognitive impairment in the cART era: a review. AIDS. 2011; 25:561–75. [PubMed: 21160410]

Sippy BD, et al. Increased expression of tumor necrosis factor-alpha receptors in the brains of patients with AIDS. J Acquir Immune Defic Syndr Hum Retrovirol. 1995; 10:511–21. [PubMed: 8548330]

Thames A, et al. B-85Genotype, CSF Inflammation, and Cognitive Performance among African Americans and European Americans with HIV-infection. Arch Clin Neuropsychol. 2014; 29:568–9.

Thompson KA, et al. Correlation between neurological progression and astrocyte apoptosis in HIV-associated dementia. Annals of Neurology. 2001; 49:745–752. [PubMed: 11409426]

Tyor WR, et al. A model of human immunodeficiency virus encephalitis in scid mice. Proc Natl Acad Sci U S A. 1993; 90:8658–62. [PubMed: 8378344]

Verstovsek S, et al. A double-blind, placebo-controlled trial of ruxolitinib for myelofibrosis. N Engl J Med. 2012; 366:799–807. [PubMed: 22375971]

Author Manuscript

Author Manuscript

Author Manuscript

Author Manuscript
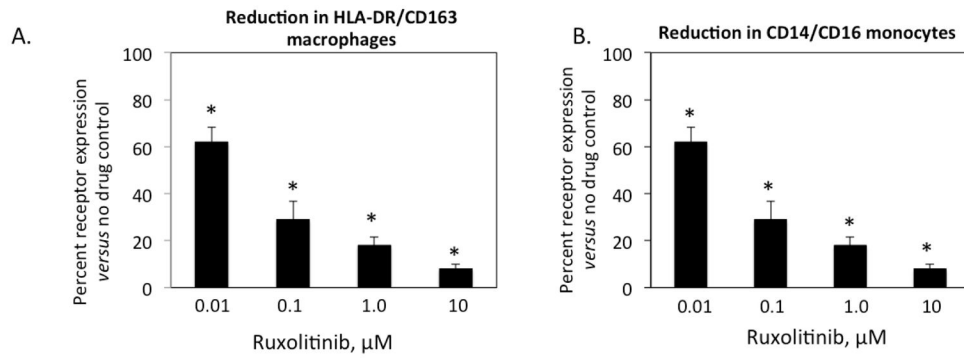
Figure 1. Ruxolitinib inhibits HIV-induced activation in primary human macrophages
(A) and monocytes (B). Ruxolitinib conferred a dose dependent reduction of activation markers that were up-regulated by HIV-1 infection in primary human macrophages (A) and monocytes (B). Data are mean and standard deviations from at least three independent experiments. * Indicates significant reduction *versus* no drug controls, $p < 0.05$, One Way ANOVA. All values are mean $\pm$ SD.
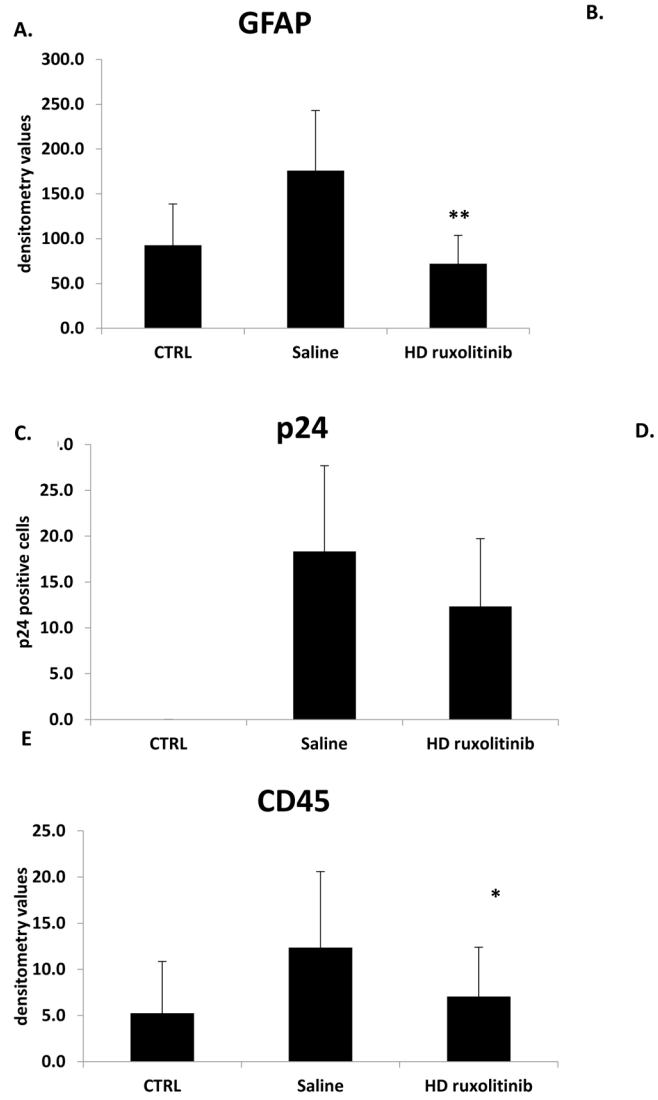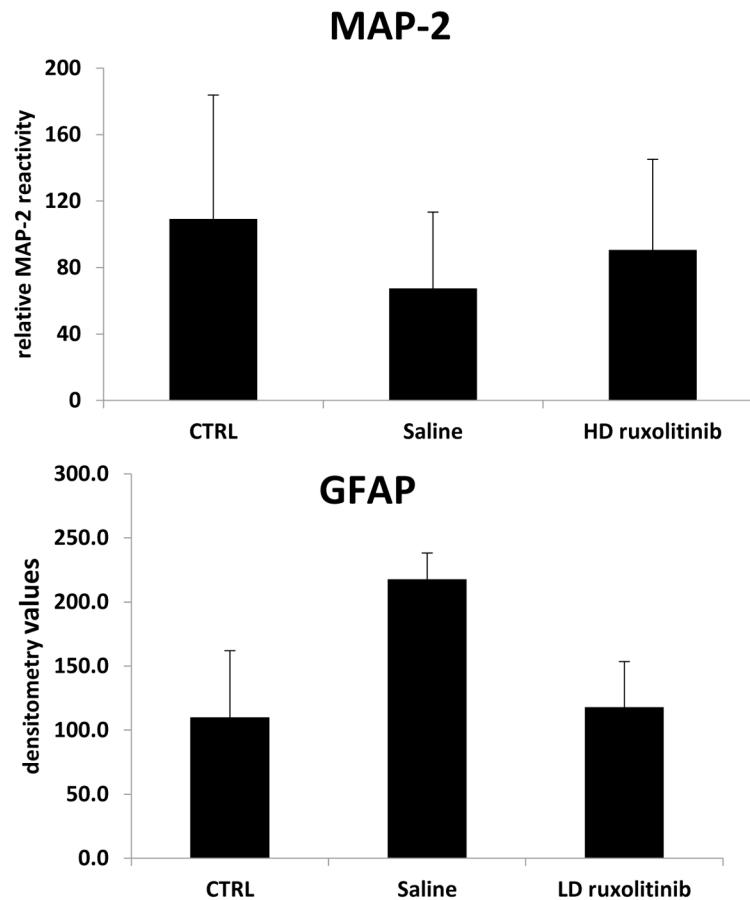
A.

GFAP

B.

C.

p24

D.

E

CD45

Figure 2a

MAP-2

GFAP

Figure 2b

Figure 2. Ruxolitinib decreases encephalitis markers in the brain in a mouse encephalitis model
High dose (HD) ruxolitinib (50 mg/kg per injection) significantly reduced astrogliosis (A), and showed a trend in the reduction of microgliosis (B) and viral load (C), and a trend for improvement of neuronal dendritic structure (D). Low dose (LD) ruxolitinib also significantly reduced astrogliosis (E). Analyses of densitometry values were performed using 1-way ANOVA and an unpaired t-test in GraphPad Prism 5 for Windows (GraphPad Software). Statistical analysis of activation markers were performed using a One Way ANOVA followed by a post-hoc test, while t-test was used to compare mean values between saline treated and ruxolitinib treated HIV-infected mice. Six mice were used for each treatment condition. *=p<0.05 and **=p<0.01 were used to denote significant differences between saline treated and ruxolitinib treated HIV infected mice. All values are mean ± SD.
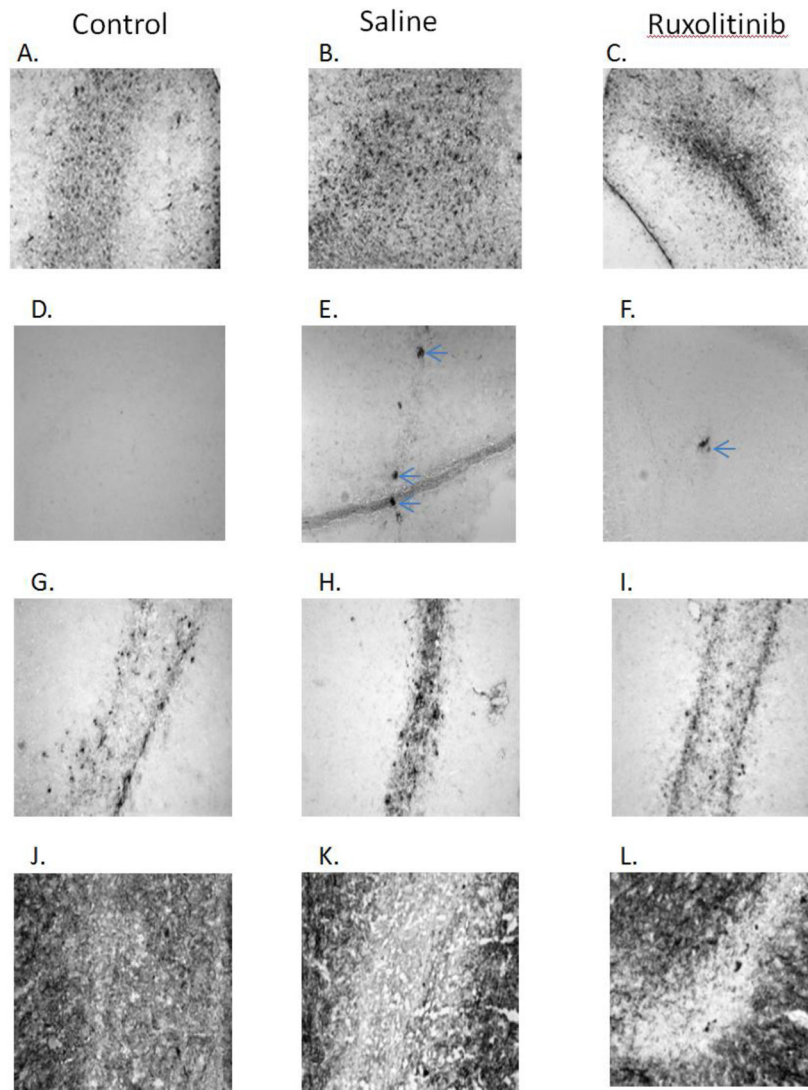
Figure 3. Representative photomicrographs showing decrease in GFAP, CD45 as well as p24 positive cells but increase in MAP-2 staining after treatment with high dose ruxolitinib
Mice treated with ruxolitinib (50 mg/kg per injection) were sacrificed 10 days post infection. Brains were extracted and 5 μm coronal sections were stained, viewed under a light microscope and imaged for astrogliosis marker, GFAP (A–C), viral burden p24 (D–F), mononuclear phagocytes marker, CD45 (G–I) and dendritic arborization marker, MAP-2 (J–L).

Table 1

Ruxolitinib concentrations in the brain of mice treated with high-dose ruxolitinib (50 mg/kg per injection)

Posterior fossa from 6 mice were homogenized and drug levels were measured by tandem mass spectroscopy. All six mice receiving high dose ruxolitinib demonstrated quantifiable concentrations of the drug in the posterior fossa that were harvested during steady-state pharmacokinetics of drug treatment. Concentrations ranged from 34.1–247.2 ng/g of tissue.

Sample #	Ruxolitinib (ng/g)
1	133.9
2	247.2
3	34.1
4	139.2
5	141.8
6	130.2